

3D coordination polymer of copper (II)–potassium (I): Crystal structure and thermal decomposition kinetics

Xiao-Qing Shen^{a,b,c}, Hai-Bin Qiao^b, Zhong-Jun Li^b, Hong-Yun Zhang^{b,*}, Hong-Lei Liu^b,
Rui Yang^b, Pei-Kun Chen^b, Hong-Wei Hou^b

^a College of Material Engineering, Zhengzhou University, Zhengzhou 450052, China

^b Department of Chemistry, Zhengzhou University, Zhengzhou, 450052, China

^c College of Chemistry, Northeast Normal University, Changchun 130024, China

Received 10 July 2005; received in revised form 11 October 2005; accepted 11 October 2005

Available online 28 November 2005

Abstract

A new heterometallacrown coordination polymer $[\text{K}_2\text{Cu}(\text{NPA})_2(\text{H}_2\text{O})_4]_n$ (where H_2NPA = 3-nitro-phthalic acid) has been synthesized and its crystal structure has been elucidated. In the complex, the *o*-phthalate group coordinates to metal atoms behaving as both tetradentate and heptadentate coordination, the modes of which have been found for the first time. The thermal behaviors of this complex and the thermal decomposition kinetics have been studied. Kinetic analysis shows that the decomposition of title complex in the main range acts as two separate transitions with the first one being a double-step following reaction, $\text{A} \xrightarrow{\text{F}_1} \text{B} \xrightarrow{\text{F}_2} \text{C}$, and the second being a three-step following reaction of t:f,f, $\text{A} \xrightarrow{\text{F}_2} \text{B} \xrightarrow{\text{F}_2} \text{C} \xrightarrow{\text{R}_2} \text{D}$. The kinetic parameters of these processes were also obtained.

© 2005 Elsevier B.V. All rights reserved.

Keywords: Copper complexes; Crystal structure; Thermal behaviors; Kinetics

1. Introduction

Metal coordination polymers containing carboxylate ions as the organic spacer have received considerable attention in the past few years due to their fascinating architectures and their advantageous properties such as bulk magnetic behavior, high dimensionality and optical activity and thermal stability [1].

Study on the synthetic methods, structures and properties of metal coordination polymers consolidated by dicarboxylate groups is particularly of interest [2–7], because “dicarboxylic acids have additional coordination abilities for the formation of new types of polymers and oligomers, which can considerably influence the magnetic, optical or catalytic properties of the ultimate products” [2].

In constructing coordination polymers, aromatic dicarboxylic acids such as *p*-phthalic, *m*-phthalic and *o*-phthalic acids are extensively used [8–11]. Among these isomeric forms the *o*-phthalate ligand, with two carboxylic groups in ortho-position, can bind metal ions in the most diverse bonding modes [7] leading to the formation of polynuclear complexes ranging from discrete entities to multi-dimensional systems. So far many metal coordination polymers with *o*-phthalic acid, including copper (II) [6,7,12], cobalt (II) [6,7,13], and zinc (II) [2,7,14], have been studied. These compounds revealed the monodentate as well as chelating and bridging bonding modes of *o*-phthalate coordination.

Recently in an effort to explore the copper (II) mixed-ligand complex with *o*-phthalate and malonate, we obtained a novel copper (II)–sodium (I) heterometallacrown compound $[\text{Na}_2\text{Cu}(\text{PA})_2(\text{H}_2\text{O})_2]$ (H_2PA = *o*-phthalic acid) [15], in which all the four oxygen atoms in one *o*-phthalate participate in coordination, with two oxygen atoms bridging one sodium and one copper atoms, another

* Corresponding author. Tel.: +86 37167763675; fax: +86 37167761744.
E-mail address: wzhy917@zzu.edu.cn (H.-Y. Zhang).

one bridging two sodium atoms and the fourth coordinating one sodium atom. In an extension of the study in this paper we report on the synthesis and single crystal structure of a new copper (II)–potassium (I) heterometallacrown complex $[K_2Cu(NPA)_2(H_2O)_4]_n$, where $H_2NPA = 3$ -nitro-phthalic acid. Thermogravimetry (TG) and differential scanning calorimetry (DSC) have been used to characterize the complex and to study the thermal behaviors during heat-treatment. Based on the results of TG and DSC, the kinetic parameters of thermal decomposition have been calculated by employing Ozawa–Flynn–Wall equation and the reaction models have been derived by means of non-linear regression method. The results and information obtained from thermal analysis can help us understand the structure and properties of $[K_2Cu(NPA)_2(H_2O)_4]_n$, and also provide basic data for further application research of this coordination polymer.

2. Experimental

2.1. Materials

All chemicals, purchased from Zhengzhou Chemical Reagent Company, were of analytic reagent grade and used without further purification.

2.2. Synthesis of complex $[K_2Cu(NPA)_2(H_2O)_4]_n$

An aqueous solution of $CuCl_2$ (2 ml, 0.5 mol L^{-1}) was added with continuous stirring to 60 ml of water containing 0.334 g (2.0 mmol) of 3-nitro-phthalic anhydride. 0.5 mol L^{-1} KOH solution were added into above-mentioned solution to keep $pH = 7$. The resulting solution was heated under stirring to reflux for 4 h and then cooled to room temperature. After two months, 0.258 g (Yield 40.8%) bright blue crystals of title complex suitable for X-ray diffraction were obtained by being filtrated, washed with cooled water and dried under vacuum. IR (KBr pellet, cm^{-1}): 3374s, 3088w, 1616vs, 1539s, 1462m, 1383s, 1349s, 1300w, 925m, 717m. Anal. Calc. for $C_{16}H_{14}N_2O_{16}CuK_2$: C, 30.38; H, 2.42; N, 4.63. Found: C, 30.44; H, 2.48; N, 4.66%.

2.3. Experimental equipment and conditions

The single crystal structure was measured on a Rigaku-Raxis-VI X-ray diffractometer using graphite-monochromated $Mo \text{ K}\alpha$ radiation ($\lambda = 0.71073 \text{ \AA}$) at 293(2) K, 3399 reflections were measured over the ranges $1.42 \leq \theta \leq 24.99$, $-8 \leq h \leq 8$, $0 \leq k \leq 12$, $-17 \leq l \leq 17$, yielding 3399 unique reflections. Raw data were corrected and the structure was solved using the SHELX-97 program. Non-hydrogen atoms were located by direct phase determination and subjected to anisotropic refinement [16]. The full-matrix least-squares calculations on F^2 were applied on the final refinement. The refinement converged at $R_1 = 0.0406$ and $wR_2 = 0.0879$ values for reflections with

Table 1

Crystal data and structure refinement parameters for $[K_2Cu(NPA)_2(H_2O)_4]_n$

Empirical formula	$C_{16}H_{14}CuK_2N_2O_{16}$
Formula weight	632.03
Crystal system, space group	triclinic, $P\bar{1}$
a (Å)	7.4264(15)
b (Å)	10.434(2)
c (Å)	14.864(3)
α (°)	104.58(3)
β (°)	92.95(3)
γ (°)	90.27(3)
V (Å ³)	1113.0(4)
Z	2
D_c (g cm^{-3})	1.886
μ (mm^{-1})	1.443
Crystal size (mm)	$0.2 \times 0.18 \times 0.18$
θ Range (°)	1.42–24.99
Reflections collected/unique	3399/3399 [$R_{\text{int}} = 0.0000$]
Final R indices [$I > 2\sigma(I)$]	$R_1 = 0.0406$, $wR_2 = 0.0879$
R indices (all data)	$R_1 = 0.0589$, $wR_2 = 0.0967$

$I > 2\sigma(I)$. Details of crystal structure determination are summarized in Table 1. Full atomic data are available as a file in CIF format.

Thermal decomposition experiments were carried out using NETZSCH TG 209 and DSC 204 instruments in N_2 atmosphere. The heating rate for thermal decomposition employed was $10 \text{ }^\circ\text{C min}^{-1}$, and the rates for kinetic analysis were 5, 10, 20 and $30 \text{ }^\circ\text{C min}^{-1}$, respectively. The IR spectra were recorded on a Nicolet IR-470 spectrometer using KBr pellets in the range of $4000\text{--}400 \text{ cm}^{-1}$.

3. Results and discussion

3.1. Description of crystal structure of $[K_2Cu(NPA)_2(H_2O)_4]_n$

Selected bond distances and angles are listed in Table 2, the structure unit is depicted in Fig. 1a, the structural core in Fig. 1b and the packing diagram of the complex in Fig. 1c, respectively.

The crystal structure of $[K_2Cu(NPA)_2(H_2O)_4]_n$ consists of a centrosymmetric polynuclear $[K_4Cu_2(NPA)_4(H_2O)_8]$ structural unit (Fig. 1a). Each Cu(II) atom in the unit has a approximately square pyramidal (CuO_5) coordination environment. For Cu1 the basal plane of the square pyramid is defined by three carboxylate-oxygen atoms (O8, O2 and O10A) belonging to three different NPA groups and one oxygen atom (O13) from a H_2O molecule. The fifth axial coordination site is occupied by one oxygen atom (O14) of bridging water ligand. The distance of Cu1 and the plane center is 0.145 \AA and four in-plane atoms, O(2), O(8), O(10A) and O(13) are almost coplanar with mean deviation from plane of 0.0144 \AA .

There are two kinds of coordination environment for potassium atoms. The K1 atom is 9-coordinated by three H_2O molecules (O15, O16, O14) and three carboxylate-oxygen atoms (O2, O3, O7) from two NPA groups in the

Table 2
Selected bond distances (Å) and angles (°) for complex $[\text{K}_2\text{Cu}(\text{NPA})_2(\text{H}_2\text{O})_4]_n$

Bond distance			
Cu(1)–O(10)#1	1.966(3)	K(1)–O(9)#4	3.171(3)
Cu(1)–O(2)	1.971(3)	K(1)–O(6)#3	2.830(4)
Cu(1)–O(13)	1.997(4)	K(2)–O(8)	2.854(3)
Cu(1)–O(8)	2.020(3)	K(2)–O(8)#1	2.841(3)
Cu(1)–O(14)	2.310(4)	K(2)–O(7)#4	2.671(3)
K(1)–O(7)	2.773(3)	K(2)–O(12)#5	2.823(4)
K(1)–O(14)	3.142(4)	C(11)–N(2)	1.469(5)
K(1)–O(1)#2	2.812(3)	O(11)–N(2)	1.214(5)
Bond angles			
O(10)#1–Cu(1)–O(14)	92.50(14)	O(16)–K(1)–O(7)	146.62(13)
O(10)#1–Cu(1)–O(8)	90.08(12)	O(12)#5–K(2)–O(9)	154.38(10)
O(10)#1–Cu(1)–O(2)	170.74(11)	O(10)#1–K(2)–O(8)#1	72.05(9)
O(3)–K(1)–O(1)#2	129.26(10)	K(2)#1–O(1)–K(1)#6	87.82(9)
O(7)#4–K(2)–O(8)#1	147.28(9)	Cu(1)#1–O(10)–K(2)#1	102.41(12)
O(7)#4–K(2)–O(8)	95.80(10)	Cu(1)–O(14)–K(1)	89.41(12)

Symmetry transformations used to generate equivalent atoms: #1 $-x, -y + 1, -z$ #2 $x + 1, y, z$ #3 $-x + 1, -y + 2, -z + 1$ #4 $-x + 1, -y + 1, -z$ #5 $x, y - 1, z$ #6 $x - 1, y, z$.

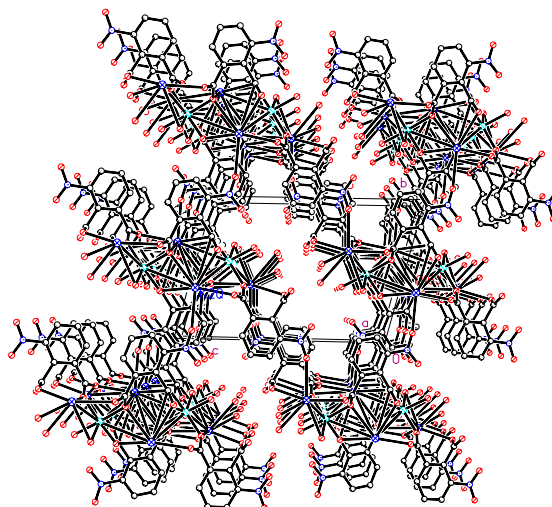


Fig. 1c. The packing of $[\text{K}_2\text{Cu}(\text{NPA})_2(\text{H}_2\text{O})_4]_n$.

(Fig. 1b). The K2 atom is 7-coordinated by five carboxylate-oxygen atoms (O8, O9, O8A, O1A, O10A) from three NPA groups within the same structural unit (Fig. 1a), as well as one carboxylate-oxygen atom (O7) and one nitro-oxygen atom (O12) of two NPA groups belonging to the other structural unit (Fig. 1b). The difference between Cu–O bond and K–O bond results from the disparity in bonding characteristic of copper and potassium atoms. The copper atom can accept the electron pair from oxygen atom forming Cu–O coordination bond, while the potassium atom forms the K–O bond through the electrostatic attraction of K^+ for O^{2-} or polar H_2O molecule. As the electrostatic attraction has no saturation level and directionality, K^+ can interact with the electronegative groups around it as more as possible and exhibit high coordination numbers. The K–O bonds formed between the neighboring structural units play an important role in constructing the coordination polymer.

NPA adopts two kinds of coordination mode in the complex, in one of which three of the four carboxylate-oxygen atoms in one NPA group are used to coordinate the metals acting as a tetradentate ligand apart from the nitro-oxygen atom which also participates in coordination, in the other mode all of the four carboxylate-oxygen atoms take part in coordination acting as a heptadentate ligand. In the tetradentate form of NPA group (Fig. 1a), one oxygen atom (O1) from one carboxylate group coordinates a potassium atom (K2A), and another oxygen atom (O2) from the same carboxylate group bridges a copper atom (Cu1) and a potassium atom (K1). The coordination of oxygen atom (O2) to copper atom (Cu1), together with that of oxygen atom (O1) to potassium atom (K2A), gives rise to a 1,3-bridging mode. The one oxygen atoms (O3) of another carboxylate group also coordinates the K1 atom forming a 1,6-chelating mode together with oxygen atom (O2). This kind of coordination mode, which can be shown by structure representation I (Scheme 1), has not been reported in the literature [7].

Fig. 1a. ORTEP drawing of $[\text{K}_2\text{Cu}(\text{NPA})_2(\text{H}_2\text{O})_4]$ unit (with 50% probability displacement ellipsoids).

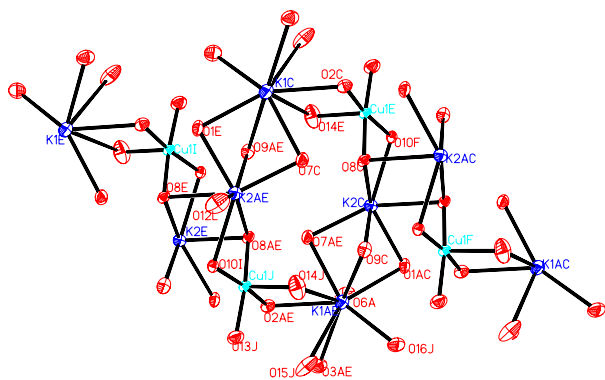
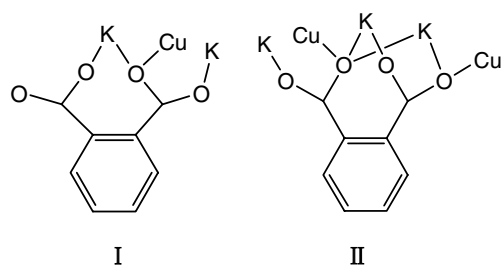


Fig. 1b. Core of the complex along a -axis.

same structural unit (Fig. 1a), as well as two carboxylate-oxygen atoms (O1, O9) and one nitro-oxygen atom (O6) of two NPA groups belonging to the other structural unit



Scheme 1.

In the heptadentate form of NPA group (Fig. 1a), one oxygen atom (O7) from one carboxylate group coordinates K1 atom, and another oxygen atom (O8) from the same carboxylate group bridges Cu1, K2 and K2A atoms. The one oxygen atom (O9) of another carboxylate group also coordinates the K2 atom forming a 1,6-chelating mode together with oxygen atom (O8), and the remaining oxygen atom (O10) bridges Cu1A and K2A atoms. The coordination of oxygen atom (O10) to copper atom (Cu1A), together with that of oxygen atom (O9) to potassium atom (K2), leads to a 1,3-bridging mode, and the coordination of O10 and O8 atoms to K2A atom at the same time forms a 1,6-chelating mode. The *o*-phthalate group acts as heptadentate coordination to metal centers forming two seven-membered cycles using 1,6-chelating mode. This kind of coordination mode, which can be shown by structure representation II (Scheme 1), has also not been reported in the literature [7].

Water coordinates to metal ions in two fashions, in one of which water (O14) is linked to two metal atoms (Cu1 and K1) behaving as a bridging ligand, in another one each water (O13, O15, O16) coordinates one metal atom (Cu1 or K1). There are two kinds of hydrogen bond formed between and within the structural units, one of which is formed between H₂O molecules, and another one between carboxylate-oxygen atoms and H₂O molecules. The hydrogen bonds formed between the structural units provide extra stability to the coordination polymer structure.

A special characteristic of this crystal structure is that four potassium atoms (K1C, K2AE, K1AE and K2C) and two copper atoms (Cu1E and Cu1J) from adjacent structural units build a 6-center metallocycle through bridging carboxylate-oxygen atoms, in which K2AE, Cu1J, K2C and Cu1E atoms are in the same plane, while K1C and K1AE atoms are slightly out of it with mean deviation from the main plane both of 0.2109 Å. The metallocycle extends to form a metal framework along *a*-axis direction (Fig. 1b). This structure is analogous to the previously reported copper (II) complex [15], but in this complex each K atoms can also link nitro-oxygen atoms of neighboring units at K(2)–O(12)#5 distance of 2.823(4) Å and K(1)–O(6)#3 distance of 2.830(4) Å to form a grid structure extending along benzene ring plane. This arrangement leads to form tunnel cavities with the biggest hole diameter of 19.065 Å in the assembled 3D polymer crystal (Fig. 1c).

3.2. Thermal decomposition and non-isothermal kinetics of $[K_2Cu(NPA)_2(H_2O)_4]_n$

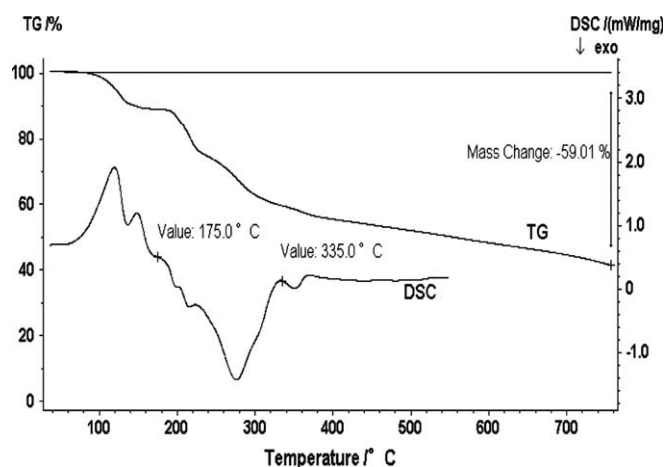
3.2.1. Thermal decomposition

The typical TG and DSC curves of title complex are shown in Fig. 2. It can be seen that there are three transitions appeared in the decomposition process. The first transition, which starts from 85 °C and ends at 175 °C, giving total ΔH value of 375.5 J g⁻¹ with two endothermic peaks at 121.1 and 148.9 °C, is due to the loss of coordinated H₂O from $[K_2Cu(NPA)_2(H_2O)_4]_n$. The calculated mass loss of 11.35% for this thermal event agrees well with that revealed by the TG curve (11.34%).

The second transition, which ranges from 175 to 335 °C, is a consecutive complicated process containing three exothermic peaks at 198.1, 215.3 and 276.7 °C. This thermal event, giving total ΔH value of -731.1 J g⁻¹ (DSC curve) with mass loss of 29.18%, is due to the decomposition of $[K_2Cu(NPA)_2]_n$ and accompanied by the formation of CuO [7] and KOCN. The third transition is beyond 335 °C and is related to the gradual elimination of carbon deposition resulted from $[K_2Cu(NPA)_2]_n$ decomposition in N₂ atmosphere [17]. The total mass loss up to 760 °C is 59.0%, which agrees with the theoretical value (60.4%) calculated by taking KOCN and CuO as the final products.

The characterization frequencies of the IR spectra of $[K_2Cu(NPA)_2(H_2O)_4]_n$ and the decomposed products at 335 and 760 °C confirmed the deduction above. The peaks at 1523 and 1500 cm⁻¹ in the IR spectrum of the complex, which are assigned to the characteristic vibration band of benzene rings, disappear in the spectrum of the decomposed products, and a new characteristic absorption peak of OCN⁻ appears at 2223 cm⁻¹ in the spectrum of both the decomposed products.

It is of interest to further investigate the enthalpy changes of this complex in first transition. Two overlapped endothermic peaks appeared in DSC curve (see Fig. 2) with the peak temperatures at 121.1 and 148.9 °C, giving total ΔH value of 375.5 J g⁻¹, correspond to the removal of

Fig. 2. TG and DSC curves of $[K_2Cu(NPA)_2(H_2O)_4]_n$.

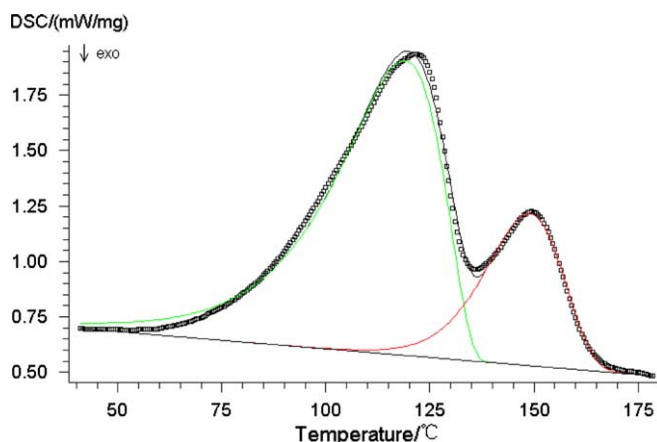


Fig. 3. Peak-separation of first transition of DSC curve.

Table 3
Peak-separation result for the first transition of decomposition

Shape	Position (°C)	Onset (°C)	Endset (°C)	Area (J mol ⁻¹)
1	118.9945	84.137	134.999	277.5173
2	148.9254	126.779	164.158	98.6287

mono-coordinated water and bridging water, respectively. We use the peak-separation technology to calculate the ΔH value of each peak. The calculated curves are presented in Fig. 3 and the calculated results shown in Table 3. The ΔH values given for these two endothermic areas are 277.5 and 98.6 J g⁻¹, respectively. $\Delta H_1/\Delta H_2 \approx 3:1$ agrees with the ratio of the number of mono-coordinated water and bridging water. That is to say, two types of coordinating mode result in these water being lost at different temperatures and the heat absorbed is proportional to the number of water molecules eliminated. On the other hand this conclusion also indicates that DSC measurement can provide a valuable way to infer unknown coordination modes of water.

From the thermal analysis above it can be seen that the main process of the decomposition of $[\text{K}_2\text{Cu}(\text{NPA})_2(\text{H}_2\text{O})_4]_n$ occurs within the temperature range of 85–335 °C. In order to simplify the problem only this temperature range would be taken into consideration in the following kinetic analysis.

3.2.2. Non-isothermal kinetics of $[\text{K}_2\text{Cu}(\text{NPA})_2(\text{H}_2\text{O})_4]_n$

A series of dynamic scans with different heating rates results in a set of data, which exhibits the same degree of conversion (α) at different temperatures. Fig. 4 shows the thermal decomposition curves of title complex at heating rates of 5, 10, 20 and 30 °C min⁻¹ in N₂ atmosphere. The basic data (β, α, T) taken from the TG curves are used in the equations below:

Ozawa–Flynn–Wall equation [18],

$$\ln \beta = \ln \left(\frac{AE}{R} \right) - \ln g(\alpha) - 5.3305 - 1.052 \cdot \frac{E}{RT}, \quad (1)$$

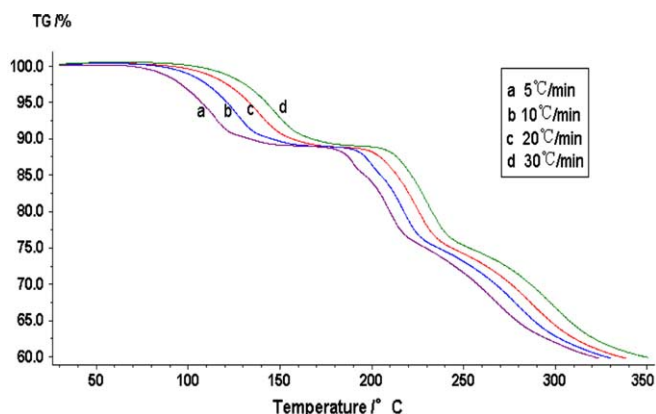


Fig. 4. TG curves with different heating rates. Heating rates listed are setting values.

where β is the heating rate, α the degree of conversion, $g(\alpha)$ the mechanism function, E the activation energy, A the pre-exponential factor and R the gas constant.

From Eq. (1) it can be seen that the graphs $\ln \beta$ versus $1/T$ show straight lines with slopes $m = -1.052E/R$. The slopes of these straight lines are directly proportional to the reaction activation energy (E). The calculated results of the first and the second transition by using Eq. (1) are listed in Table 4.

The dependence of E on α given in Table 4 shows that the activation energy is not a constant and two maximums appear at $\alpha = 0.05$ and 0.9 for first transition and three maximums at $\alpha = 0.3, 0.6$ and 0.9 for the second, which indicates that the thermal decomposition of $[\text{K}_2\text{Cu}(\text{NPA})_2(\text{H}_2\text{O})_4]_n$ can be separated into a double-step and a three-step reaction, respectively [19]. According to OFW method, the activation energies and pre-exponential factors of thermal decomposition for the first transition are, $E_1 = 71.4$ kJ mol⁻¹, $E_2 = 97.8$ kJ mol⁻¹, respectively; for second transition, the values of these parameters are $E_1 = 154.8$ kJ mol⁻¹, $E_2 = 173.1$ kJ mol⁻¹, $E_3 = 216.2$ kJ mol⁻¹, respectively. These values would offer initial values for getting reaction

Table 4
Parameters E (kJ mol⁻¹) and $\lg(A/s^{-1})$ for main thermal decomposition of $[\text{K}_2\text{Cu}(\text{NPA})_2(\text{H}_2\text{O})_4]_n$

Partial mass loss (α)	First transition		Second transition	
	E (kJ mol ⁻¹)	$\lg(A/s^{-1})$	E (kJ mol ⁻¹)	$\lg(A/s^{-1})$
0.02	71.43 ± 9.43	7.89	139.76 ± 11.38	12.21
0.05	66.54 ± 5.61	6.65	135.46 ± 7.20	11.93
0.10	54.47 ± 3.57	4.89	135.57 ± 4.35	12.04
0.20	44.70 ± 2.43	3.50	154.84 ± 5.79	14.20
0.30	41.04 ± 2.14	3.01	158.48 ± 5.88	14.55
0.40	40.15 ± 2.15	2.91	158.08 ± 7.15	14.39
0.50	40.91 ± 2.34	3.04	173.07 ± 14.34	15.53
0.60	42.69 ± 2.74	3.32	160.62 ± 12.15	13.77
0.70	45.14 ± 3.45	3.70	163.69 ± 11.63	13.78
0.80	50.06 ± 4.87	4.41	170.56 ± 12.70	14.20
0.90	71.36 ± 10.89	7.16	198.47 ± 24.25	16.49
0.95	97.77 ± 19.56	10.65	216.17 ± 37.34	17.84
0.98	88.36 ± 16.09	9.33	214.67 ± 43.92	17.51

Table 5
Kinetic parameters and fitting quality after NLR method

Transition	Corr. coeff.	Reg. par.	Step	E (kJ mol ⁻¹)	lg(A/s^{-1})	Order
1st	0.999836	0.00100	I F1	78.67363	8.22818	0.74
			II F_n	102.90499	11.93783	
2nd	0.999817	0.00100	I F2	157.21424	16.85279	
			II F2	184.2119	15.2992	
			III R2	215.7978	17.8387	

model by means of non-linear regression (NLR) and would be optimized finally.

Non-linear regression [20] allows a direct fit of the model to the experimental data without a transformation and there are no limitations with respect to the complexity of the model. For this reason, NLR method can be employed for estimating the decomposition model of $[K_2Cu(NPA)_2(H_2O)_4]_n$. Selecting mechanism function $f(\alpha)$ of different singular reaction types [21]; testing all double-step and three-step reaction types to which individual steps are linked for the first and second transition, respectively [21]. Setting the initial values of the parameters of E and lgA according to OFW method, the calculated curves were obtained by means of NLR. These curves were fitted to the experimental ones and corrected with LSQ. During this procedure in order to get high fitting quality kinetic parameters of initial values are optimized. Considering fitting quality (characterized by correlation coefficient), the mechanism of d:f, $A \xrightarrow{F1} B \xrightarrow{F_n} C$, is the most suitable for water loss reaction. And the mechanism of t:f,f, $A \xrightarrow{F2} B \xrightarrow{F2} C \xrightarrow{R2} D$, for the decomposition of $[K_2Cu(NPA)_2]_n$. The kinetic parameters and statistical characterization after the NLR are listed in Table 5, graphic presentation of the curve fitting for the second transition are presented in Fig. 5, which shows that the experimental data and the non-linear regression curves fit very well.

In short, the result of the kinetic analysis above shows the mechanism of $[K_2Cu(NPA)_2(H_2O)_4]_n$ decomposition:

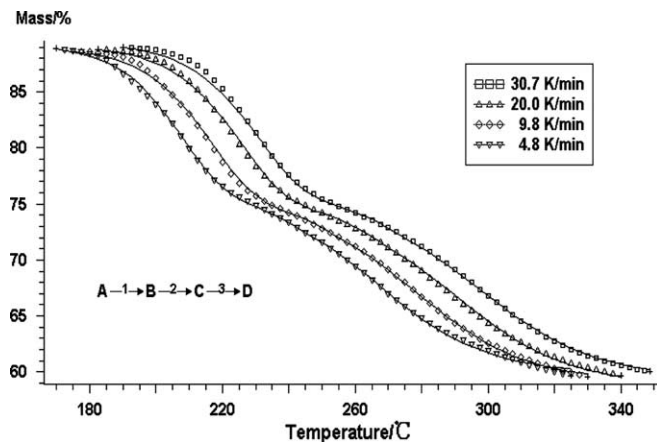


Fig. 5. Curve fitting of second transition, simulated with reaction types F2, F2 and R2. ∇ , \diamond , Δ , \square experimental plots, – integral plots. Heating rates listed are measured values.

the first transition assigned to water loss is a double-step following reaction: an 1st-order reaction (F1) is followed by an n th reaction (F_n) with $n = 0.74$; The second transition responsible for main decomposition of $[K_2Cu(NPA)_2]_n$ preferably performs as a three-step following reaction: two following 2nd-order reactions (F2) are followed by a 2-dimensional phase boundary reaction (R2).

4. Conclusions

- Complex $[K_2Cu(NPA)_2(H_2O)_4]_n$ shows *triclinic* structure with space group $P\bar{1}$. The crystal structure consists of a centrosymmetric polynuclear structural unit. Cu(II) atom has a approximately square pyramidal (CuO5) coordination environment and four potassium atoms together with two copper atoms build a 6-center metal-cycle through bridging carboxylate-oxygen atoms along a -axis. In this complex, the *o*-phthalate group coordinates to metal atoms behaving as tetradentate and heptadentate coordination, the modes of which have not been reported in the literature.
- Thermal analysis indicates that the process of $[K_2Cu(NPA)_2(H_2O)_4]_n$ decomposition includes two transitions. First transition is assigned to the loss of coordinated water, the second corresponds to the decomposition of $[K_2Cu(NPA)_2]_n$. Two types of coordinating mode result in the coordinated H_2O being lost at different temperatures and the heat quantity absorbed is proportional to the number of water molecules eliminated.
- Kinetic analysis shows the mechanism of $[K_2Cu(NPA)_2(H_2O)_4]_n$ decomposition: the first transition is a double-step following reaction, $A \xrightarrow{F1} B \xrightarrow{F_n} C$, with $E1 = 78.7$ kJ mol⁻¹, $lg(A1/s^{-1}) = 8.2$; $E2 = 102.9$ kJ mol⁻¹, $lg(A2/s^{-1}) = 11.9$, $n = 0.74$; The second transition is a three-step following reaction, $A \xrightarrow{F2} B \xrightarrow{F2} C \xrightarrow{R2} D$, with $E1 = 157.2$ kJ mol⁻¹, $lg(A1/s^{-1}) = 16.9$; $E2 = 184.2$ kJ mol⁻¹, $lg(A2/s^{-1}) = 15.3$; $E3 = 215.8$ kJ mol⁻¹, $lg(A3/s^{-1}) = 17.8$.

5. Supplementary material

Supplementary crystallographic data have been deposited with the Cambridge Crystallographic Data Center, CCDC No. 228386. Copies of this information may be obtained free of charge on application to The Director, 12 Union Road, Cambridge CB2 2EZ, UK (fax: +44

1223 336033; e-mail: deposit@ccdc.cam.ac.uk or <http://www.ccdc.cam.ac.uk>).

Acknowledgements

We thank the Natural Science Foundation of China (20271046), the Natural Science Foundation of Henan Province (0211020300) and the Natural Science Foundation of Henan Education Department (2004150004) to provide financial support.

References

- [1] P.S. Subramanian, D. Srinivas, *Polyhedron* 15 (1996) 985.
- [2] S.G. Baca, Yu.A. Simonov, N.V. Gerbelev, M. Gdaniec, P.N. Bourosh, G.A. Timco, *Polyhedron* 20 (2001) 831.
- [3] J.L. Tian, S.P. Yan, D.Z. Liao, Z.H. Jiang, P. Cheng, *Inorg. Chem. Commun.* 6 (2003) 1025.
- [4] Y. Qua, Y.X. Kea, S.M. Lu, R. Fan, G.Q. Pan, J.M. Li, *J. Mol. Struct.* 734 (2005) 7.
- [5] B. Zurowska, J. Mrozinski, *Inorg. Chim. Acta* 342 (2003) 23.
- [6] S.G. Baca, S.T. Malinovskii, P. Franz, C. Ambrus, H. Stoeckli-Evans, N. Gerbelev, S. Decurtins, *J. Solid State Chem.* 177 (2004) 2841.
- [7] S.G. Baca, I.G. Filippova, O.A. Gherco, M. Gdaniec, Yu.A. Simonov, N.V. Gerbelev, P. Franz, R. Basler, S. Decurtins, *Inorg. Chim. Acta* 357 (2004) 3419.
- [8] C.S. Hong, Y. Do, *Inorg. Chem.* 36 (1997) 5684.
- [9] L. Li, D. Liao, Z. Giang, S. Yan, *Inorg. Chim. Acta* 357 (2004) 405.
- [10] M. Eddaoudi, J. Kim, J.B. Wachter, H.K. Chae, M. O'Keeffe, O.M. Yaghi, *J. Am. Chem. Soc.* 123 (2001) 4368.
- [11] D.R. Whitcomb, R.D. Rogers, *Inorg. Chim. Acta* 256 (1997) 263.
- [12] N.V. Gerbelev, Yu.A. Simonov, G.A. Timco, P.N. Bourosh, J. Lipkowski, S.G. Baca, D.I. Saburov, M.D. Mazus, *Russ. J. Inorg. Chem.* 44 (1999) 1191.
- [13] Yu.A. Simonov, M. Gdaniec, I.G. Filippova, S.G. Baca, G.A. Timco, N.V. Gerbelev, *Russ. J. Coord. Chem.* 27 (2001) 353.
- [14] S.G. Baca, I.G. Filippova, N.V. Gerbelev, Yu.A. Simonov, M. Gdaniec, G.A. Timco, O.A. Gherco, Yu.L. Malaestean, *Inorg. Chim. Acta* 344 (2003) 109.
- [15] H.L. Liu, H.Y. Mao, H.Y. Zhang, C. Xu, Q.A. Wu, G. Li, H.W. Hou, *Polyhedron* 23 (2004) 943.
- [16] G.M. Sheldrick, *Acta Crystallogr., Sect. A* 46 (1990) 467.
- [17] X.Q. Shen, H.J. Zhong, H.Y. Zhang, H.Y. Mao, Q.A. Wu, Y. Zhu, *Polyhedron* 23 (11) (2004) 876.
- [18] T. Ozawa, *Bull. Chem. Soc. Jpn.* 38 (1965) 1881.
- [19] S. Vyazovkin, *Int. J. Chem. Kinet.* 28 (1996) 95.
- [20] P.D.M. Benoit, R.G. Ferillo, A.H. Ganzow, *Anal. Chim. Acta* 124 (1985) 869.
- [21] C.H. Bamford, C.F. Tipper (Eds.), *Comprehensive Chemical Kinetics*, vol. 22, Reactions in Solid State, Amsterdam, 1980, p. 57.